Effect of Water Mist on a Confined Blast

by

Ramagopal Ananth[1], Harold D. Ladouceur, Heather D. Willauer,
John P. Farley, and Fredrick W. Williams
Chemistry Division
Naval Research Laboratory
Washington, DC 20375
(ramagopal.ananth@nrl.navy.mil)

Abstract

A computational, multi-phase, model has been developed to study the dynamics of the interactions between water droplets and radial expansion of a gas cloud in a spherical chamber. Initial conditions for the gas cloud are specified based on chemical equilibrium calculations for the detonation of a high explosive (RDX). Mono-dispersed water droplets are injected at uniform concentration into the chamber prior to the expansion. A Lagrangian model is used to track the breakup of the parent drops near the shock front to form child drops. The Navier-Stokes solutions show that the child droplets accumulate near the shock front and evaporate at 100 times higher rate than the parent droplets. Latent heat absorption is the dominant mechanism followed by the sensible heat absorption by the water vapor (and droplets), and momentum absorption from the high velocity gases by the child droplets. The simulations also show that the water vapor formed by the evaporation increases the gas density at the shock front. The increased density and reduced gas temperature (cooling) have opposite effects on the pressure at the shock front. This leads to only a modest suppression in the pressure. At realistic concentrations (80 gm/m^3), the water mist is shown to evaporate completely in a short time prior to shock reflection at the chamber wall mainly due to the breakup at the shock front. High concentration of mist may be desirable, but are difficult to achieve in practice at the total flooding conditions.

Introduction

Fine water droplets have been shown to be very effective in suppressing fires by absorbing latent and sensible heats and by diluting the oxygen needed for combustion [1]. Computational and experimental studies [2-4] were used to determine the minimum mist concentrations needed to extinguish a diffusion flame for a given droplet size (3 – 200 μm) under ideal mist flow conditions. Large-scale studies [5] on the ex-USS Shadwell show that when water mist is dispersed at roughly uniform concentration (total flooding) engulfing the fire, the fire can be extinguished. The U.S. Navy has implemented a fixed, total flooding, water mist technology on a new class of ships for fire suppression. The goal of the present work is to investigate the effects of fine water mist on detonation of high explosives.

Detonations of high explosives such as TNT or RDX involve combustion reactions, which occur on extremely small time scales because the fuel molecule contains a significant portion of the oxygen needed for combustion. However, the subsequent expansion of the hot combustion gases (fireball) over a length of few meters inside the confines of a Navy vessel can occur at a relatively slow pace (milliseconds). Furthermore, a shock front is formed in front of the thermal front (fireball) by the expanding gases. The shock is reflected back and forth by the compartment walls multiple times over a period of hundreds of milliseconds. Therefore, fine water droplets dispersed into the compartment prior to the blast may not inhibit the primary

[1] To whom correspondence should be addressed, (202) 767-3197

combustion, but can potentially interact with the shock and the expanding fireball to cause suppression.

Sommerfeld [6] studied the mitigating effects of inert particles on a blast wave created by a small pressure gradient in a shock tube. He showed that glass particles slow down the shock propagation significantly due to inertia and heat capacity at high concentrations (20 -66% by mass). Therefore, the main mechanism of mitigation by the inert particles is due to momentum absorption from the supersonic gases. Joseph et al [7] studied water droplets introduced into a shock tube and elucidated the fragmentation phenomena caused by the shear forces. The pressure gradient employed in the shock tube studies were significantly smaller than those created typically by the high explosives. Catlin [8] performed mitigation experiments using bulk water placed near the explosive so that water is atomized by the blast. Keenan and Wagner [9] showed 90 % reduction overpressure caused by a TNT blast by water bags. Van Wingerden [10] studied the mitigation of gas explosions using water sprays. Buzukov [11] examined the effects of a water curtain on air shock. Very few studies have been performed on the interaction of small water droplets on detonation of high explosives.

We have conducted large scale tests [12] using 2 to 7 lbs of TNT placed at the center of 65 m^3 bombproof chamber at the Naval Surface Warfare Center (NSWC), Indian Head, Maryland . The charges were detonated after fine water mist was sprayed into the chamber using high pressure nozzles. These tests showed about 30-40% reduction due to the water mist in the quasi-static (smoothed) overpressure in the chamber. Recently, we have also conducted larger scale tests (50 lbs TNT equivalent) in a 180 m^3 chamber using TNT, PBXn109, and Destex explosives [13]. Fine water mist was sprayed for 30 seconds to achieve a roughly uniform spatial distribution (total flooding)

Schwer and Kailasanath [14-16] simulated some of our smaller tests by performing Eulerian computations of the water droplets. They considered small charges of TNT (5 lbs) detonated inside spherical and cylindrical chambers. To our knowledge, these are the first simulations of their kind to understand the blast mitigation. They showed significant mitigation of the overpressure for large water concentrations, 30 to 70 mass % and 10-50 μm droplet diameters. The droplets were assumed to remain intact at the shock front without fragmentation. Their simulations suggested that the momentum absorption from the gas phase by the droplets is the main mechanism of suppression. Adiga et al [17] performed thermodynamic calculations of the energy absorption due to the increased surface area resulting from fragmentation of the droplets at the shock front. Adiga et al suggested that the surface energy absorption by itself was small but the child droplets could have significantly higher evaporation rates than the parent droplets. Ananth et al [18] performed thermodynamic calculations of the overpressure due to the reaction between Aluminum metal contained in the explosives and the water mist assuming well-mixed, closed, adiabatic conditions. Ananth et al [18] showed that the generation of water vapor and cooling of the combustion gases have opposite effects on the overpressure.

Water droplets suspended in air can interact with the blast by several mechanisms: (1) the droplets slow down the expanding gases due to their inertia by absorbing some of the kinetic energy, (2) Some of the energy transferred from the gas to the droplet is used up in increasing the total surface area (or total surface energy [19]) upon the droplet breakup at the shock front, (3) thermal radiation absorption by the water droplets, (4) absorption of the sensible heat needed to heat the water to boiling temperature, (5) absorption of the latent heat by droplet evaporation, (6) absorption of additional sensible heat due to higher specific heat of water vapor than air, (7) the water vapor formed by evaporation of droplets dilutes the oxygen, which is needed by secondary combustion reactions (slow reaction between excess fuel and ambient oxygen; e.g., TNT contains

60% of stoichiometric oxygen, therefore, fuel is left over after the primary combustion), (8) on the other hand, the water vapor formed can also increase the gas density, which increases the overpressure and counteracts the suppression by the water droplets. The precise mechanisms of interactions of water droplets with a blast and their relative importance remain unclear. In this work, we consider the effects of increased evaporation rates due to fragmentation suggested by Adiga et al. [17] for a blast caused by 50 lbs high explosive inside a 3.5 m radius spherical chamber. Because of the large mass of the explosive, the temperature at the shock front can be high. Therefore, the thermal mechanisms of water mist suppression can be significant and will be elucidated by simulations with and without the droplet fragmentation in the current paper.

Analysis

In this paper, we solve time dependent, compressible, Navier-Stokes equations in a spherically symmetric geometry to describe the expansion dynamics of the shock front and the fireball. The computational domain is chosen to be a sliver (5^0 angle), which is a small section of the spherical domain, because of the spherical symmetry. The sphere radius is 3.5 m. The computational domain is discretized along the radial direction (r), and the other two directions are one cell wide. An isothermal (298 K) wall boundary conditions is imposed at r=3.5 m. We also solve the multiphase droplet equations to describe the interaction of the water mist with the gas phase using a Lagrangian approach. Initially, mono-dispersed water droplets of specified diameter are injected uniformly into the air contained in the chamber for a short time to establish a uniform mass concentration of water (total flooding) throughout the chamber. A reflecting wall boundary is imposed for the droplets.

We assume a 0.3 m radius fireball is formed instantly under adiabatic conditions at the center of the spherical chamber upon detonation of a 35 lbs RDX (50 lbs TNT equivalent). Therefore, chemical thermodynamic calculations for a constant volume explosion inside the fireball were performed using the CHEETAH 4.0 code [20], which was developed by Lawrence Livermore Laboratory. In these equilibrium calculations, the Chapman-Jouget (CJ) detonation state and the adiabatic expansion of the gases to 0.3 m radius spherical volume are obtained. CHEETAH 4.0 [19] uses appropriate empirical equations of state and predicts the pressure, temperature, and density in the 0.3 m radius spherical volume for the RDX detonation. Based on these calculations, uniform pressure and temperature are specified to be about 2000 atm and 4000 K respectively inside the 0.3 m fireball. This establishes the initial conditions for the dynamic computations of subsequent fireball-expansion inside the spherical chamber containing water mist.

The Navier-Stokes and the energy equations are solved in conjunction with ideal gas law to predict the changes in pressure, temperature, and density with time and radial position during the fireball expansion into the mixture of air and water mist. This is done using the FLUENT software package [21]. The equations contain source/sink terms, which are evaluated by solving the droplet phase equations. Gas density depends both on pressure and temperature for compressible flow with the ideal gas law. The thermodynamic and transport properties are temperature, pressure, and composition dependent, and are calculated using ideal-gas mixing law and kinetic theory of gases. During the fireball expansion, the CO mixes with the oxygen in ambient air and reacts to produce CO_2 (secondary reaction) at a slow rate. For 35 lbs RDX, CO has to mix with 32 lbs of air for complete combustion. Even though the secondary reaction has the potential to release a large amount of energy, the energy release rate depends mainly on the rate of mixing at the thermal front. The rate of mixing occurs initially by diffusion over a distance of 0.5 m and later due to significant number of shock reflections, which cause turbulence. The diffusion time scale is of the order of 100 seconds. Therefore, the mixing occurs on seconds time scale even with turbulence. Indeed, Schwer and Kailasanath concluded that the

oxygen dilution effects on the secondary reaction is not significant. Also, for some explosives such as nitroglycol and nitroglycerine, the oxygen content is more or less balanced, and no fuel is left to react during the expansion phase. Therefore, we neglect the secondary reaction kinetics during the fireball expansion over a short time (<< 1 sec) before a significant turbulence is generated by the shock reflections.

The droplet phase equations describe mass, momentum and energy balances for each droplet injected. The Lagrangian approach is used to obtain the evolution of droplet position, velocity, temperature, and diameter with time. The droplet energy balance includes the droplet heating and evaporation. The droplet evaporation rate includes the mass transfer effects for the water vapor at the surface, heat transfer effects, and the vapor-liquid equilibrium thermodynamics effects. Behind the shock front, the water droplets are exposed to supercritical conditions (T_c=647.2 K and P_c = 218 atm). A vapor pressure curve up to the critical point is used in the calculation of the droplet evaporation rate. Therefore, the droplet is allowed to heat to the critical point before reaching a boiling state. A lumped parameter spherical drag and heat transfer (Newton's law of cooling) models are used to describe momentum, mass, and heat exchange between gas and the droplet. An average constant diffusivity ($D_{H2O,m}$=1.5 x 10^{-5} m^2/sec) is used in the Sherwood number calculation.

G.I. Taylor's droplet breakup model [22] is used. In this model, the analogy to a damped, spring oscillator is made to account for the droplet distortion due to the drag and viscosity forces imposed by the gas stream and the surface tension force. Breakup is assumed to occur when the distortion in shape reaches the radius of the parent drop. Child droplet size and number are obtained from the energy and mass balances before and after the breakup event. We have also performed calculations using a wave model of Reitz [23] based on Kelvin-Helmholtz instability. The wave model did not show significant differences from the Taylor model for the pressure and temperature fields. However, the wave model exhibited oscillations and are computationally expensive. Initially, only one drop per cell is tracked. As the droplets break, the number of droplets tracked increases. However, as the droplets evaporate completely, the number tracked decreases with time. Each droplet tracked corresponds to a parcel of drops of uniform size, velocity, temperature, and position. The parcel size depends on the mass concentration of the mist. The parameters computed for a tracked droplet is multiplied by the parcel size to obtain source/sink terms, which appear in the gas phase equations.

The numerical computations were performed using the FLUENT 6.3.26 package with 3500 uniform cells of 1 mm size placed along the radius of the sliver. A time marching technique with a time step of 0.05 to 0.2 μsec, and an implicit finite volume numerical method are used for the calculations. The discreet phase model (DPM) and Taylor's breakup model contained in FLUENT are used for the water mist. A user defined function (DEFINE_ON_DEMAND) file was written in C language for the uniform injection of the mono-dispersed droplets of specified size, position, and zero velocity to achieve the total flooding conditions in the sliver. Unsteady particle tracking is performed at every time step. A SGI Altix 3700 parallel machine consisting of Intel Itanium 2 processors (1.6 GHz each) is used through DOD's High Performance Computing Resources. A typical CPU time is 13 hours with a run time of 30 hours for 12000 time steps using 30 processors.

Results and Discussion

Initially, the pressure, temperature, velocity, and specie CO_2 and H_2O vapor mass fractions are uniform for radius, r, less than or equal to 0.3 m, and are set at 2000 atm, 4000 K, 0,

0.89 and 0.11 respectively. Ambient conditions are assumed for r>0.3 m. Initially, the water droplets are of uniform diameter, d_0, and concentration, C_{0w}, for all values of r. The pressure and thermal fronts coincide at r=0.3 m and t=0. As the fireball expands, the pressure or shock front propagates ahead of the thermal front, and all the quantities change with r and time, t. Next, we show Navier-Stokes results at a time prior to reaching the wall of the closed spherical chamber.

Figure 1 shows pressure, temperature, water droplets, and water vapor distributions for C_{ow}=0.08 Kg/m^3, d_0=50 µm, and t=2.13 msec. The concentration and drop diameters are based on the measurements reported by Willauer et al [13] in the blast mitigation tests conducted recently at the Naval Surface Warfare Center (NSWC), Indian Head, MD. Figure 1a shows the shock front, where the pressure decreases sharply from its peak value to atmospheric pressure in the undisturbed air ahead of the shock. It shows that the shock front is located at r=3.13 m. Figure 1b shows the temperature distribution and the thermal front, which is located at 2.47 m. Behind the thermal front, the temperatures are high (1500 K), and the product species mass fractions are

Figure 1a. Pressure Contours

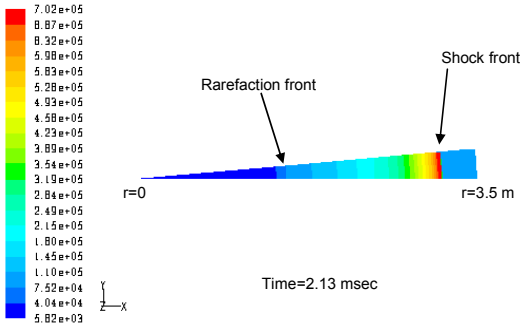

Figure 1b. Temperature Contours

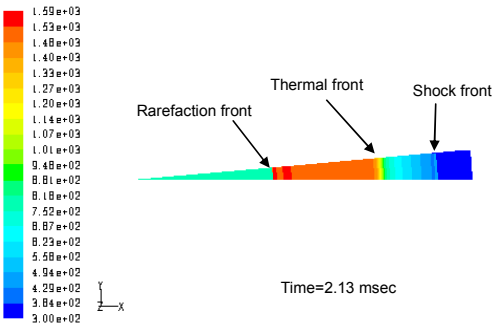

Figure 1c. Water Mist Contours

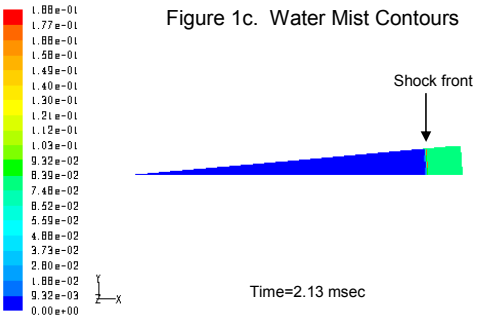

Figure 1d. Water Vapor Contours

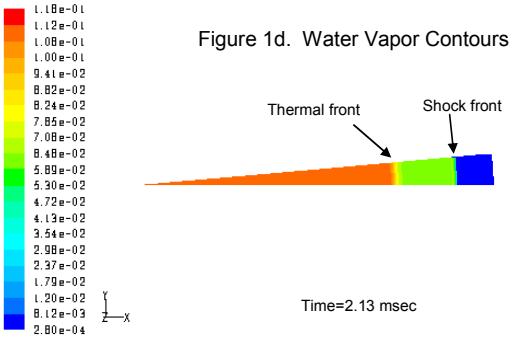

at their initial values. There is very little mixing between the product species from the primary reaction and the ambient air at the thermal front during the short period of 2.13 msec. Between the thermal and shock fronts, the temperature decreases to a relatively low value (500 K), but is significantly higher than the ambient and can cause water evaporation. In this region, the product species mass fraction is zero. Figure 1c shows that the water droplets are pushed by the expanding gases and concentrated to a very narrow region (shown in yellow) just behind the shock front. In this region, the concentration reaches its peak value and decreases sharply to its initial value (0.08) in the undisturbed air ahead of the shock front. Figure 1d shows that the water droplets are evaporated only in the region between the thermal and shock fronts to form water vapor mass fraction of 0.066. There is no droplet evaporation behind the thermal front because the water vapor mass fraction is identical to the initial value (0.11) specified for the product specie. Clearly, water droplets do not get inside the thermal core. However, they evaporate

completely between the thermal and shock fronts. Indeed, the simulations show that very little liquid water is left in the chamber after the shock front reaches the spherical wall located at r=3.5 m. Therefore, in this paper, we focus on the effects of droplet breakup and evaporation prior to its reflection at the wall.

As the water droplets enter behind the shock front (r=3.13 m), they are broken up by the extremely high gas velocities. Figure 2 shows simulations with and without the breakup for the mist concentration distribution just behind the shock front. With the breakup, the droplets are concentrated within a short distance (3 cm) behind the shock. Without the breakup, the droplets spread 45 cm behind the shock. This is because of sharp reduction in the droplet diameters from

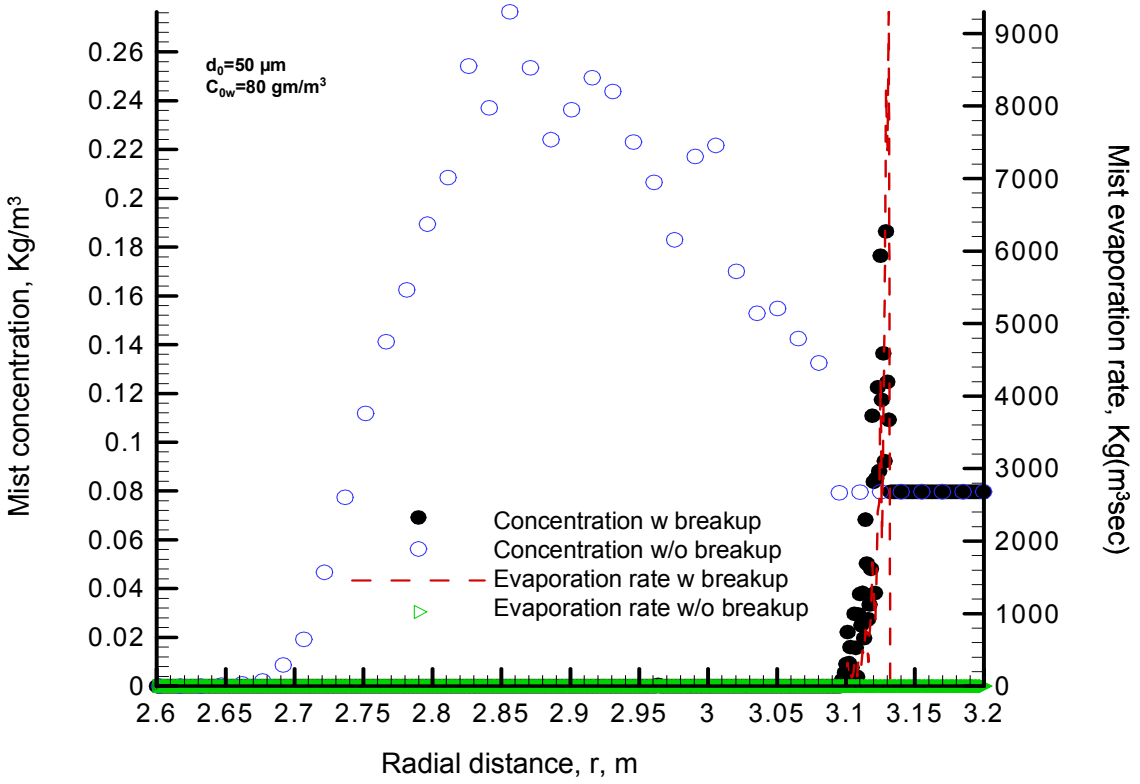

Figure 2. Comparison of mist concentration and evaporation rates with and without droplet breakup

50 µm to less than 2.5 µm caused by the breakup as shown in Figure 3. This sharp reduction in size increases the mist evaporation rate by orders of magnitude as shown by comparing the evaporation curves with (the broken red line) and without (square symbols near the abscissa) the breakup in Figure 2. Figure 3 also shows that the droplet diameter decreases slowly from 50 µm to 10 µm over a significant distance due to evaporation without the breakup. Figure 3 shows that the droplets reach their maximum temperature and velocity at a shorter distance from the shock front with the breakup than without the breakup.

Figure 4 compares different mechanisms of energy absorption rates by the droplets without the droplet breakup. The latent heat absorption rate due to the droplet evaporation is the dominant

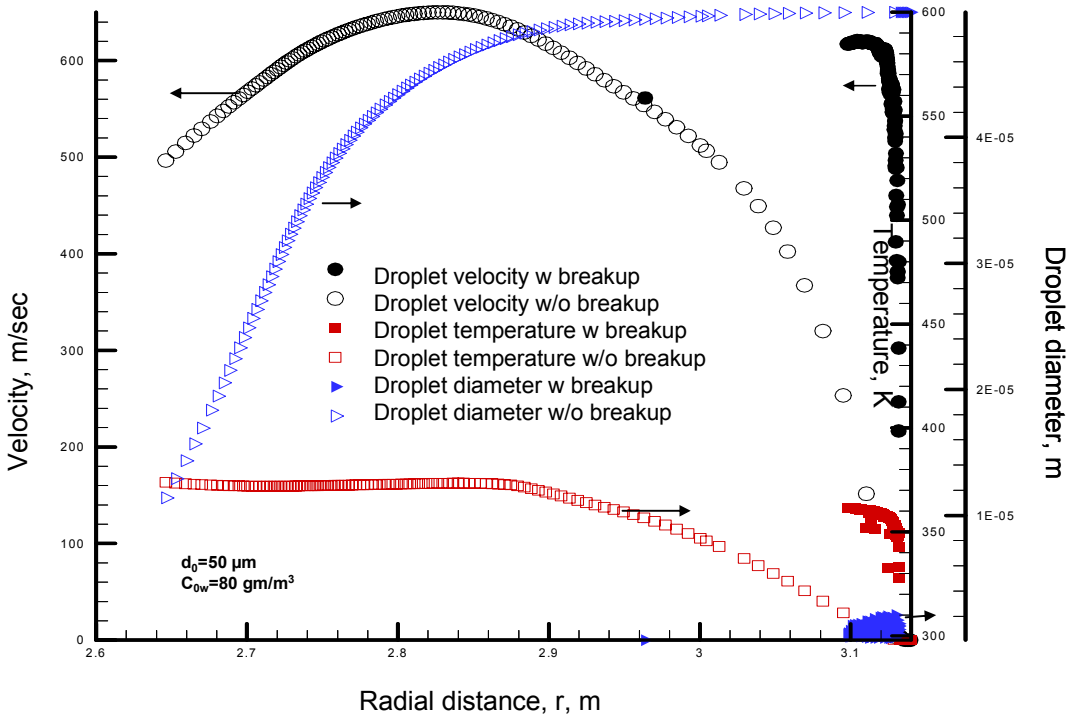

Figure 3. Comparison of droplet variables with and without the breakup

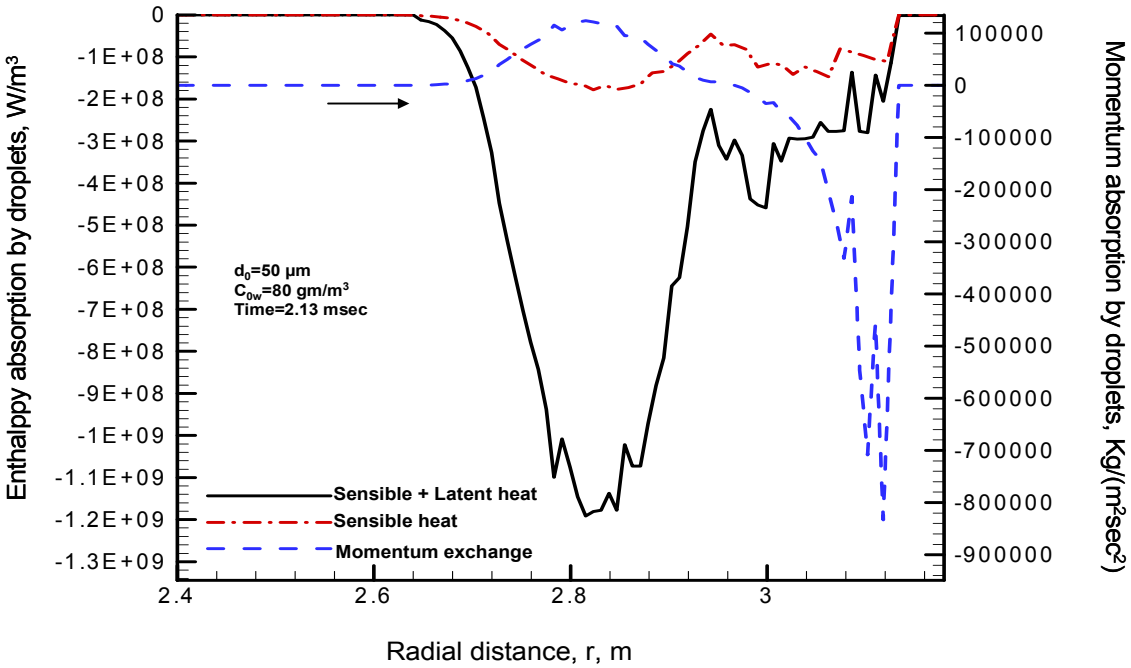

Figure 4. Energy and momentum absorption by droplets without breakup

mechanism by which energy is removed from the gases in the region between the thermal and shock fronts. The sensible heat absorption rate is about 20 % of the latent heat absorption rate. The sensible heat includes heating of both the water vapor formed by evaporation to the gas temperature and the liquid water to the evaporation temperature. Figure 4 also shows the momentum absorption rates, which occur mainly close to the shock front. The peak momentum absorption rate (-8.5 x 10^5 Kg/(m^2s^2)) can be converted to kinetic energy by multiplying with the velocity difference between the droplets and the gas. For a velocity difference of 300 m/sec, the peak kinetic energy absorption is 2.55 x10^8 W/m^3, which is comparable to the sensible heat absorption rate.

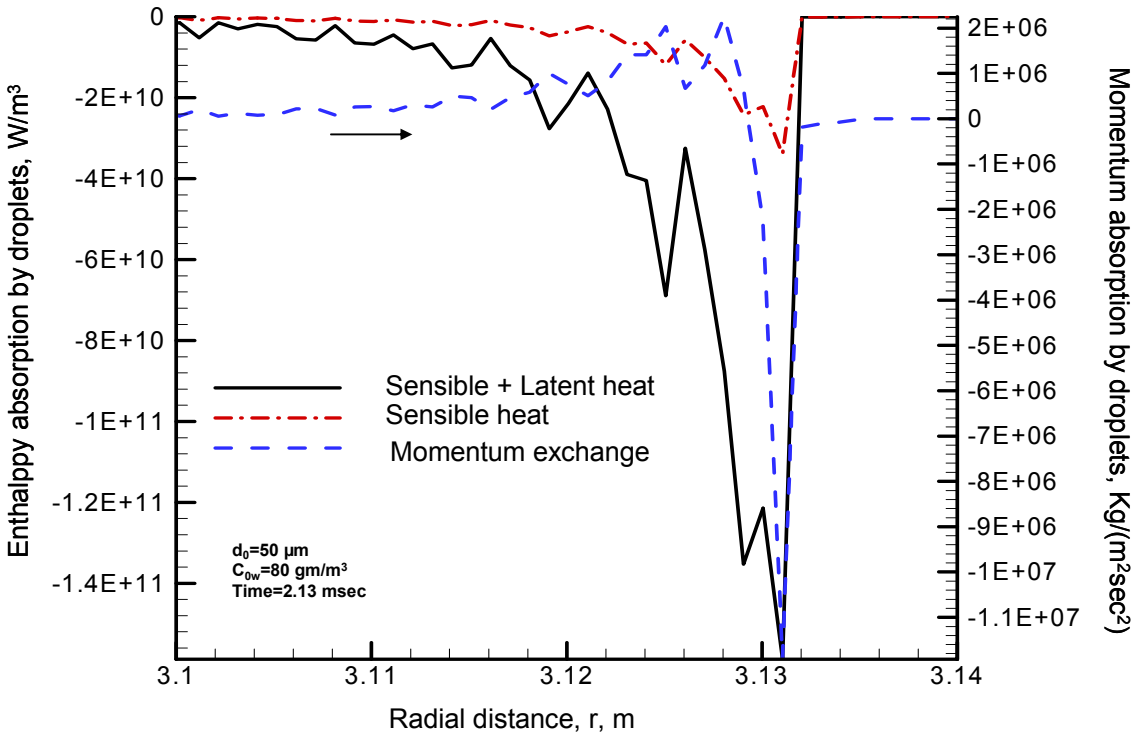

Figure 5. Energy and momentum absorption with droplet breakup

Figure 5 compares different paths for energy absorption by the droplets with the droplet breakup. The droplet break up increases the sensible and latent heat energy absorption rates by more than a factor of 100 when compared with the rates shown in Figure 4. Also, the momentum absorption rates are increased by the breakup phenomena by a factor of 10 or more. The latent heat absorption by the mist evaporation remains by far the dominant mechanism. Sensible heat absorption due to droplet and water vapor heating is about 30% of the latent heat absorption based on the peak rates. However, the momentum absorption rates are about 10 times less than the sensible heat absorption, unlike the case without the breakup, where both the mechanisms are comparable. This is because the droplets are close to the shock front with the droplet break up (shown in Figure 2), where the gas velocities are significantly lower than farther away from it. Clearly, the droplet breakup enhances the energy absorption by the mist significantly.

Water mist (with breakup) decreases the propagation velocity of the shock front by about 10 %. Therefore, the shock front arrives at a fixed location (r=3.13 m) with and without mist at different times, t=2.13 msec and 1.93 msec respectively. This enables a comparison of the mist effects on the gas phase variables. Figure 6 shows that the gas density (black lines) increases by about 30% near the shock front due to the droplet breakup and evaporation compared to the

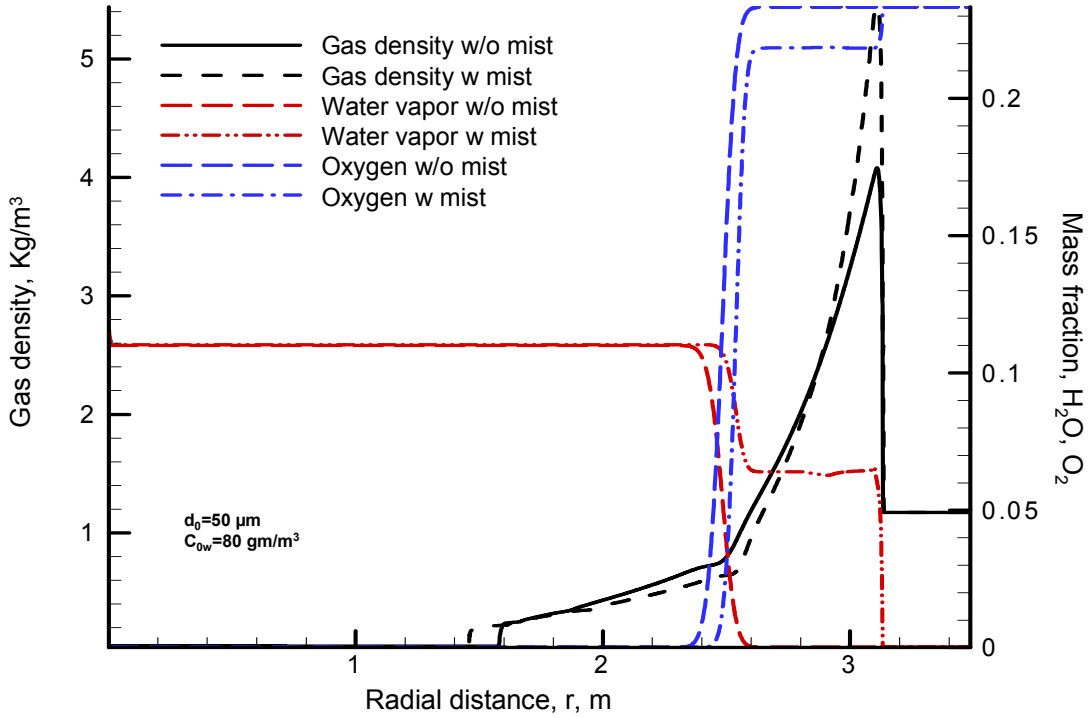

Figure 6. Effects of mist on gas density and specie mass fractions

density without the mist. This is important because it can increase the pressure, which is proportional to the density following the ideal gas law. Figure 6 also shows that the mass fraction of the water vapor generated from the mist increases sharply to 0.066 near the shock front. The water vapor dilutes the oxygen and lowers the oxygen mass fraction from 0.233 to 0.218 near the shock. At the thermal front (located at r=2.47 m), the oxygen mass fraction decreases to zero, and the water vapor mass fraction increases to the initially specified product specie concentration (0.11) for the mist case. The specie concentration gradients are less steep at the thermal front than at the shock front indicating that the mixing rate due to diffusion is slow and occurs over 0.2 m length scale. Therefore, any secondary oxidation reactions in the field may not play a significant role at the small times. Behind the shock front, the gas density decreases to near zero at the rarefaction front located at about 1.43 m. Behind the rarefaction front, temperature decreases from 1500 K to about 800 K and absolute pressure decreases below 1 atm as shown in Figure 7.

Figure 7 shows that the temperature (red lines) behind the shock front decreases by as much as 43% with the mist compared to that without the mist. Clearly, the region between the shock and the thermal fronts is relatively cool due to the water droplet breakup and evaporation. The reduced temperature should decrease the pressure significantly. However, Figure 7 shows that the pressure is decreased by only 13 % at the shock front due to the presence of the mist. This is

mainly due to the increased gas density by the droplet evaporation shown in Figure 6. Figures 6 and 7 show clearly that the water mist breakup and evaporation near the shock front has

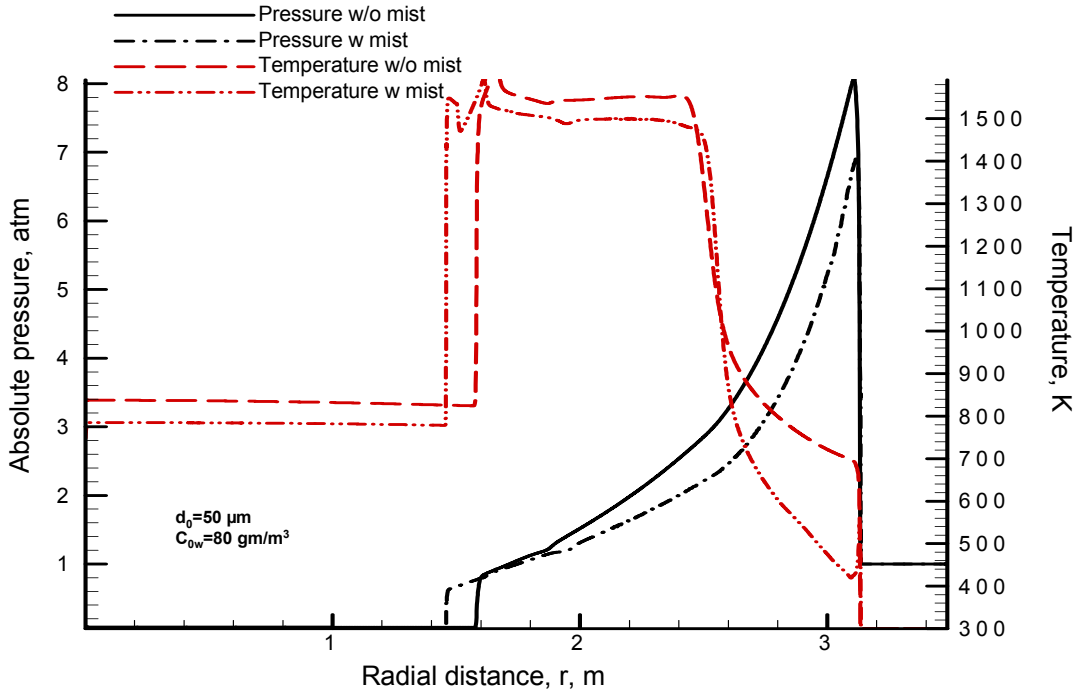

Figure 7. Effects of water mist on pressure and gas temperature

competing effects on the pressure due to the reduced temperature and the increased gas density. In our simulations without the droplet breakup, the pressure and temperature decreased by about 4 % and density remained unchanged at the shock front in the presence of the mist compared to the values without the mist. Therefore, the droplet breakup phenomena have a positive effect on the pressure reduction at the shock despite the opposite effects of reduced temperature and increased gas density.

The current predictions are interestingly similar to the previous prediction by Ananth et al [18] for 35 lbs RDX (50 lbs TNT equivalent). Ananth et al [18] performed thermodynamic calculations for the detonation of RDX in the presence of water mist mixed with air inside the spherical chamber using CHEETAH 4.0. This includes both primary and secondary reactions, and assumes complete mixing of the chamber contents to simulate the adiabatic, steady state conditions. Their simulations predicted a 12 % reduction in the quasi-static (absolute) pressure from 4.9 atm to 4.3 atm for 100 gm/m^3 mist concentration. This occurs despite a 25 % reduction in the temperature of the gases due to the increased gas density by complete evaporation of the mist to form water vapor.

The formation of the shock, thermal, and rarefaction fronts shown in Figure 1a and 1b are qualitatively similar to the computations of Schwer and Kailasanath [14-16]. However, important differences between the current work and that of Schwer and Kailasanath occur due to the neglect of droplet breakup and differences in the quantity of the explosive and mist concentration. The shock front temperature is significantly lower for the smaller charges. Schwer and Kailasanath [16] inferred from their simulations that momentum absorption by the droplets is the key mechanism for suppression of the quasi-static pressure for drops (10 to 50 µm) at very high concentrations (500-2000 gm/m^3). Without the breakup, the droplets last beyond many shock

reflections at the walls and play a significant role over a long time (1 sec) in the simulation performed by Schwer and Kailasanath [16] unlike in the current paper. Also, high concentrations of mist may be achieved locally if the water nozzles are directed at the explosive. However, only moderate (<100 gm/m^3) mist concentrations can be achieved for total flooding conditions (uniform distribution of mist) in the context of large fires and blasts in practice [13].

In the tests conducted recently by Willauer et al [13], quasi-static pressure is measured by pressure gauzes mounted near the wall in a rectangular (20' x 20' x 16') compartment for different explosives (50 lbs TNT equivalent) detonated at the center. The pressure near the wall is recorded from the time of detonation for about 2 seconds. The pressure pulses are recorded, each time the shock front approaches the wall and is reflected back. They reported 29-36% in the initial peak pressure (gauze) recorded immediately after the detonation. They also reported 33-41% reduction in the quasi-static (gauze) peak pressure, which is obtained by averaging the pressure pulses over small time-intervals. The suppression in the initial peak pressure may be compared with the suppression in the shock front pressure predicted by our computations shown in Figure 7. The computations under predict the pressure by a factor of 2.5 for 80 gm/m^3 mist concentration, which was measured in the tests for droplet sizes less than 200 μm. This is encouraging considering differences in the shape of the geometry, type of explosive, droplet size and space distributions between the tests and the theory. However, further computations are needed to understand this discrepancy by varying the mist concentration and droplet sizes. The effect of droplet sizes is expected to be small because even a 400 μm droplet is fragmented at the shock front to form extremely small child drops, which evaporate rapidly.

Conclusions

We describe the radial expansion of a high pressure, high temperature gas cloud from the center of a closed spherical chamber to its walls prior to a shock reflection. Initially, the gas cloud is generated by performing chemical equilibrium calculations for the detonation of a high explosive. Mono-dispersed water droplets are injected at a uniform concentration into the chamber prior to the expansion. The unsteady, compressible flow, Navier-Stokes computations show that the droplets are pushed by the expanding gases and accumulate behind the shock front. Latent heat absorption by evaporation is shown to be the dominant mechanism by which water droplets absorb energy near the shock front, which is at a significantly higher temperature than the ambient gas ahead of it. The droplet-breakup near the shock front is shown to enhance the energy absorption by 100 times or more and cools the gases in the region between the shock and thermal fronts significantly. However, water vapor formed from the droplet evaporation increases the gas density. This results in a small reduction in the pressure, despite a significant reduction in the gas temperature. Most of the water mist evaporates completely prior to the arrival and reflection of the shock front at the chamber wall, for an initial diameter of 50 μm and concentration of 80 gm/m^3. Large concentrations may be desirable but are difficult to achieve with the currently available total flooding technologies.

Acknowledgements

This work is supported by the Office of Naval Research through the Naval Research Laboratory. This work is also supported by a grant of computer time from the DOD HPCMP on the Aeronautical Systems Center SGI Origin 3900 and Altix 3700. We also thank Fluent Inc, Lebanon, NH for their customer support during this work.

References

1. McCaffrey, B.J., Comb. Sci. and Tech., 40, 107 (1998)
2. Ananth, R. and Mowrey, R.C., Comb. Sci. and Tech., submitted

3. Ananth, R. and Mowrey, R.C., "Ultra –fine Water Mist Extinction of a Diffusion Flame", paper# H34, 5th U.S. Combustion Meeting, San Diego, CA, March 25-28, 2007
4. Fisher, B.T., Awtry, A.R., Sheinson, R.S., and Fleming, J.W., 31st Int. Proc. Comb. Inst., 2731(2006)
5. Darwin, R.L. and Williams, F.W., "The Development of water Mist Fire Protection Systems for U.S. Navy Ships", Naval Engineers J., 112 (2000)
6. M. Sommerfeld, Experiments in Fluids, 3, 197 (1985)
7. Joseph, D.D., et al., Int. J. Multiphase flow, 25, 1263 (1999)
8. Catlin, C., J. Hazard. Mat., A94, 103 (2002)
9. Keenan, W.A. and Wager, P.C., "Mitigation of Confined Explosion Effects by Placing Water in Proximity of Explosives", 25th DOD Explosives Safety Seminar, Anaheim, CA, August 18-20, 1992
10. van Wingerden, K., Process Safety Progress, 19, 173 (2000)
11. Buzukov, A.A., Combustion, Explosion and Shock Waves, 36, 395 (2000)
12. Willauer, H.D., Bailey, J.L., and Williams, F.W., "Water Mist Suppression System Analysis", Naval Research Laboratory Letter Report 6180/0030, 7 February, 2006
13. Willauer, H.D., Ananth, R., and Williams, F.W., "Blast Mitigation using Water Mist", 32nd United States Department of Defense Explosives Safety Seminar, Philadelphia, 22-24 August, 2006
14. Schwer, D. and Kailasanath, K., "Blast Mitigation by Water Mist (1) Simulation of Confined Blast Waves", Naval research Laboratory Memo Report MR/6410-02-8636, August 16, 2002
15. Schwer, D. and Kailasanath, K., "Blast Mitigation by Water Mist; (2) Shock Wave Mitigation Using Glass Particles and Water Droplets in Shock Tubes", Naval Research Laboratory Memo Report MR/6410-03-8658, January 21, 2003
16. Schwer, D. and Kailasanath, K., "Blast Mitigation by Water Mist; (3) Mitigation of Confined and Unconfined Blasts", Naval Research Laboratory Memo Report MR/6410-06-8976, July 14, 2006
17. Adiga, K.C., Willauer, H.D., Ananth, R., and Williams, F.W., "Droplet Breakup Energies and Formation of Ultra-fine Mist", Suppression and Detection Research and Applications- A Technical working Conference (SUPDET 2007), Orlando, FL, March 5-8, 2007
18. Ananth, R., Farley, J.P., Williams, F.W., Willauer, H.D., "Thermodynamic Calculations of Overpressure Caused by the Detonation of Aluminized Explosives Inside a Closed Compartment Containing Water Mist", Naval Research Laboratory Letter Report 6180/0282, August 7, 2006
19. Levich, V.G., "Physicochemical Hydrodynamics", (translated by Scripta Inc.) Prentice Hall Inc., Englewood Cliffs, NJ 1962
20. Fried, L.E., CHEETAH 4.0 User's Manual, Lawrence Livermore National Laboratory (2006)
21. FLUENT 6.3 User's Manual, ANSYS Inc., Lebanon, NH
22. Taylor, G.I., "The shape and Acceleration of a Drop in a High Speed Air Stream", Technical Report, In the Scientific Papers of G.I. Taylor, Ed. G.K. Batchelor, 1963
23. Reitz, R.D., Atomization and Spray Technology J, 3, 309 (1987)